Photochemical & Photobiological Sciences

PAPER

View Article Online
View Journal | View Issue

Cite this: *Photochem. Photobiol. Sci.*, 2017, **16**, 1801

Femtosecond excited state dynamics of a stilbene–viologen charge transfer complex assembled *via* host–guest interaction

Mikhail V. Rusalov, *[a] Valery V. Volchkov,[a] Vladimir L. Ivanov,[a] Mikhail Ya. Melnikov,[a] Ivan V. Shelaev,[b] Fedor E. Gostev,[b] Victor A. Nadtochenko,[a,b] Artem I. Vedernikov,[c] Sergey P. Gromov[a,c] and Michael V. Alfimov[c]

Received 11th May 2017,
Accepted 18th October 2017

DOI: 10.1039/c7pp00170c

rsc.li/pps

The dynamics of the excited states of a supramolecular complex with a charge transfer between (*E*)-bis(18-crown-6)stilbene and 4,4′-(*E*)-ethene-1,2-diylbis[1-(2-ammonioethyl)pyridinium]tetraperchlorate was studied by means of femtosecond transient spectroscopy. It is found that the characteristic time of the conversion of the locally excited (LE) state into the charge transfer (CT) state is equal to 300 fs, whereas the characteristic time of the conversion of the CT state into the ground state is equal to 400 fs. Due to host–guest interaction involving hydrogen bonds, the complex possesses high thermodynamic stability. As a result of ultrafast photoinduced processes of the direct and back electron transfer, the complex does not fluoresce. Upon the interaction of the complex with alkaline-earth metal cations, "switch-on" of its fluorescence occurs.

Introduction

Bis-crown ether derivatives are of interest due to their unique properties which are absent in their monocyclic analogues.[1] The distinctive feature of bis-crown ethers is the cooperative effect of complex formation of two macrocycles. The variation of the length of the link, which separates the macrocycles, as well as its flexibility and spatial geometry enables control of this effect, and allows one to change the efficiency and selectivity of cation binding. Bis-crown ethers and their derivatives tend to form sandwich complexes with cations of large sizes. The linking of two crown-ether moieties with a flexible polymethylene or polyoxyethylene bridge leads to an increase in the stability of the complexes with K^+, Rb^+ and Cs^+ ions.[2–4] The introduction of photosensitive chemical groups into bis-crown ether structures in some cases enables photochemical control of the binding of cations. Examples of such photoactive compounds are crown-containing azobenzenes,[5–8] diarylethylenes,[9,10] or triphenylmethane.[11,12]

Another important feature of bis-crown ethers is their ability to form strong complexes with 1,ω-alkanediammonium salts.[13–17] Due to cooperative effects, the stability constants of such complexes are 5–6 orders of magnitude higher than those of the monocrown ether complexes.

Being weakly bound systems, organic charge transfer complexes (CTCs) usually possess low thermodynamic stability. In order to increase their stability, it was suggested to introduce such complexes into supramolecular ensembles with host–guest interaction. In certain ensembles huge macrocycles which can bind large organic cations such as viologen or a diazapyrenium cation were successfully used.[18–22] In some of these systems together with the coordination bond, a topological bond between the donor and acceptor rings also takes place.[23–25]

The study of the CTC between bis-crown ethers and viologen analogues bearing two terminal ammonioalkyl groups[13,26–34] is interesting for the following reasons. On the one hand, such pseudocyclic supramolecular complexes are easily formed in solution due to the self-assembly and are characterized by very high thermodynamic stability. On the other hand, they are rather labile and can react with excess of the donor or with side cations. The CTC formed between bis-crown ethers and viologen analogues are convenient objects for studying the dynamics of fast electron transfer. Previously,[29] the dynamics of photoinduced electron transfer in the CTC between (*E*)-bis(18-crown-6)stilbene (**D**) and 4,4′-(*E*)-ethene-1,2-diylbis[1-(2-ammoniopropyl)pyridinium]tetraper-

[a]*Chemistry Department, M. V. Lomonosov Moscow State University, Leninskie Gory 1-3, Moscow 119991, Russian Federation. E-mail: mvrusalov@yandex.ru; Fax: +7 (495) 9328846; Tel: +7 (495) 9391671*
[b]*N. N. Semenov Institute of Chemical Physics, Russian Academy of Sciences, Kosygina str. 4, Moscow 119991, Russian Federation. Fax: +7 (499) 1378357; Tel: +7 (495) 9397347*
[c]*Photochemistry Center, Russian Academy of Sciences, Novatorov str. 7A-1, Moscow 119421, Russian Federation. Fax: +7 (495) 9361255; Tel: +7 (495) 9350116*

chlorate was studied by femtosecond transient absorption spectroscopy. It was shown that the back electron transfer conversion of the CT state into the ground state occurs with a characteristic time of 540 fs.

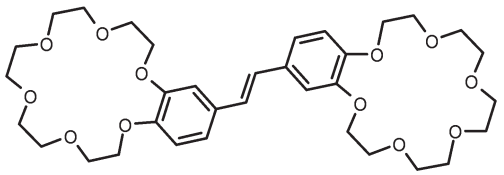

D

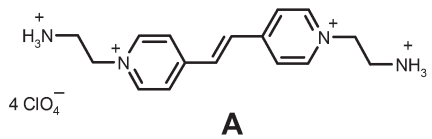

A

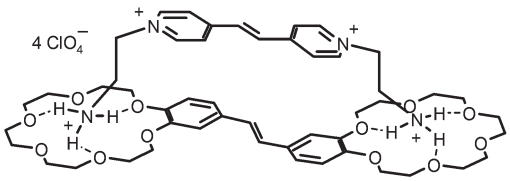

DA

In the present work we studied the dynamics of the excited state of the 1 : 1 complex (**DA**) between **D** and 4,4′-(*E*)-ethene-1,2-diylbis[1-(2-ammonioethyl)pyridinium]tetraperchlorate (**A**). Since the ammonioethyl *N*-substituents in **A** are shorter than the ammoniopropyl substituents of the acceptor applied in the previous work,[29] **DA** can be used for studying the effects of spatial separation of a donor and an acceptor of a CTC on the femtosecond dynamics of excited states and on photoinduced electron transfer.

Experimental

(*E*)-Bis(18-crown-6)stilbene (**D**) was prepared according to ref. 35. The synthesis of 4,4′-(*E*)-ethene-1,2-diylbis[1-(2-ammonioethyl)pyridinium]tetraperchlorate (**A**) was carried out as described previously.[34]

Barium and calcium perchlorates (Merck) were dried *in vacuo* (1 Pa) at 200 °C for 5 h in a VacuCell calciner. Anhydrous acetonitrile (Cryochrome, spectral grade, the water content <0.03%) was used. Solutions were prepared under the light of a red lamp to prevent the *E*–*Z*-photoisomerization of compounds **D** and **A**.

Steady-state absorption spectra were recorded on a Shimadzu-3100 spectrophotometer. Steady-state fluorescence spectra were recorded on a PerkinElmer LS-55 spectrofluorometer. Fluorescence quantum yields were determined in aerated solutions relative to a solution of quinine bisulfate in 1 N H_2SO_4 (φ = 0.546) which is used as a standard.[36]

Femtosecond transient absorption spectra were recorded on a pump and light supercontinuum probe setup with a 3.33 fs delay step and a 0.5 nm wavelength step. The details of the setup are described elsewhere.[37]

The stability constants of the complexes and the characteristic times of various excited state processes according to the polyexponential model were found using a nonlinear least squares method with the second order optimization function and Hessian numerical approximation, approaching the calculated matrix of optical densities to the experimental one.[38] The spectra of individual components were found by the linear least squares method performing matrix transformations.[29] We used the matrices of differential optical densities at delay times from 10 fs to 3 ps and with a step of 5 fs for finding characteristic times of fast processes. The matrices of differential optical densities at delay times from 5 ps to 500 ps and with a step of 1 ps were used to find the characteristic times of slow processes.

Relative errors for the values of equilibrium constants are estimated as 20%, of fluorescence quantum yields as 10%, and of the characteristic times of transient absorption dynamics as 5%.

Results and discussion

Steady-state spectroscopy

Fig. 1 shows the absorption spectra of **D**, **A** and **DA** in MeCN. A weak wide band (ε = 340 M^{-1} cm^{-1}) at 500–700 nm is an evidence of CTC formation. For comparison, the CT band intensity of a covalently bound intramolecular CTC with viologen is 15 times higher (ε = 5600 M^{-1} cm^{-1}).[39]

The interaction of bis-crown ether **D** with dipyridylethylene derivative **A**, taken in an equimolar quantity, results in the formation of a CTC (**DA**).

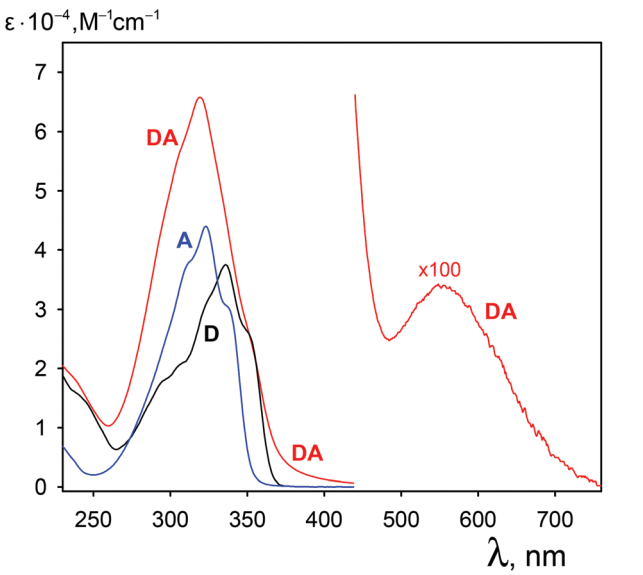

Fig. 1 Absorption spectra of **D**, **A** and **DA** in MeCN. The CT band intensity of **DA** is amplified 100 times.

$$D + A \overset{K_{DA}}{\rightleftarrows} DA \quad (1)$$

The stability constant $\log K_{DA}$, found earlier by the guest-competitor titration technique (where 1,12-dodecane-diammonium diperchlorate was a competitor), is equal to 9.42 [33] or 9.0.[34] Due to the ultrafast subpicosecond processes of the direct and back electron transfer, complex **DA** does not fluoresce as well as similar CTCs.[29,33,34] The fluorescence quenching of **D** in MeCN takes place when the acceptor **A** is gradually added (Fig. 2). The linear dependence of fluorescence intensity on the concentration of the quencher in almost all concentration ranges (Fig. 2, inset) does not allow us to determine the stability constant K_{DA} directly due to its very large value. In order to determine K_{DA} we used a guest-competitor technique where a metal cation **M** was used as a competitor. Intermediate products **DM** and **DMA** cannot accumulate in the solution without an excess of **D** or **A**, respectively. Because the stability constant of the complex of one ammonioalkyl substituent with one macrocycle is small ($\log K$ = 2.9),[31] the only product of displacement is complex $\mathbf{DM_2}$. Thus, the decomposition of **DA** by metal salts takes place according to eqn (2):

$$DA + 2M \overset{K_S}{\rightleftarrows} DM_2 + A \quad (2)$$

We studied the decomposition of complex **DA** under the influence of barium and calcium perchlorates. The decomposition of **DA** leads to the appearance of free molecule **A** and to the formation of complexes $\mathbf{DBa_2}$ and $\mathbf{DCa_2}$.

When barium salt is added, a gradual decrease in the CT band intensity takes place (Fig. 3, above). At the same time, the fluorescence enhancement also occurs (Fig. 3, below).

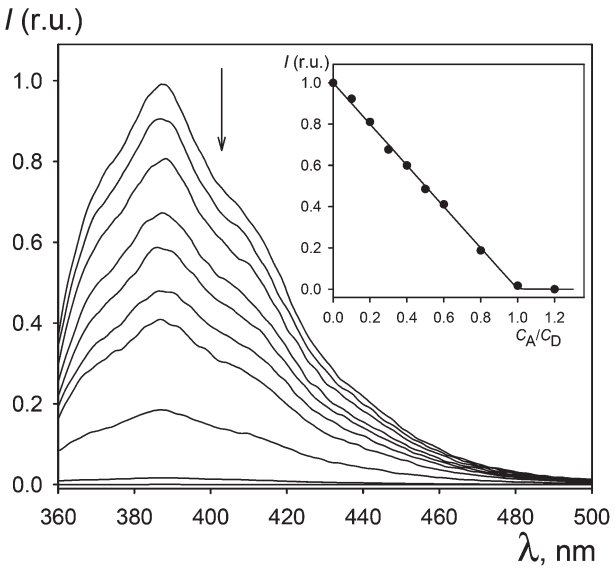

Fig. 2 Fluorescence quenching of **D** in MeCN ($C = 6 \times 10^{-6}$ M) depending on the relative concentration of **A** (C_A/C_D varies from 0 to 1.2). Excitation wavelength is 355 nm. Inset: the dependence of the fluorescence intensity of **D** at 385 nm (I) on the relative concentration of **A** (C_A/C_D). The solid line shows theoretically predicted trend obtained by using eqn (1).

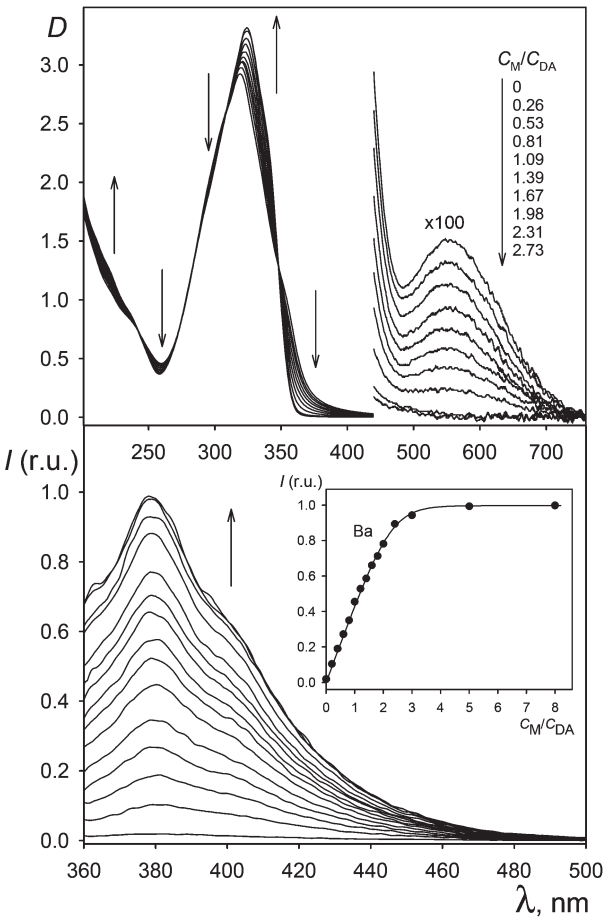

Fig. 3 Above: Absorption spectra of **DA** in MeCN ($C = 4.5 \times 10^{-5}$ M) with various relative concentrations of barium perchlorate (C_M/C_{DA} varies from 0 to 2.7). The absorption intensity at 500–700 nm is amplified 100 times. Below: Fluorescence enhancement of the solution of **DA** in MeCN ($C = 10^{-5}$ M) with a gradual increase in the relative concentration of barium perchlorate (C_M/C_{DA} varies from 0 to 8). The excitation wavelength is 349 nm. Inset: The dependence of fluorescence intensity at 380 nm (I) on the relative concentration of barium perchlorate (C_M/C_{DA}). The solid line shows the theoretical dependence obtained from eqn (2).

In order to obtain the stability constant K_{DA} from the substitution constant K_S of **A** by two metal cations, it is necessary to know the product K_1K_2 of the formation constants at the first and the second stages of the process.

Then K_{DA} can be obtained from eqn (3):

$$\log K_1 + \log K_2 = \log K_S + \log K_{DA} \quad (3)$$

The interaction of **D** with metal cations takes place as follows:

$$D + M \overset{K_1}{\rightleftarrows} DM \quad (4)$$

$$DM + M \overset{K_2}{\rightleftarrows} DM_2 \quad (5)$$

and leads to the formation of complexes **DM** and $\mathbf{DM_2}$.

The formation of sandwich complexes for bis(18-crown-6) stilbene is not observed except for a very large Cs^+ cation.[40,41]

In spite of several isosbestic points being observed upon the spectrophotometric titration of the solution of **D** with barium perchlorate (Fig. 4), this system contains three components rather than two components, as evidenced by the rank of the optical density matrix according to Wallace–Katz.[42] The stepwise character of complexation is clearly observed in the fluorescence spectra, because the intermediate complex **DM** fluoresces weakly. Upon addition of calcium perchlorate to the solution of **D**, at first fluorescence quenching takes place due to the formation of complex **DCa**, which is followed by fluorescence enhancement due to the formation of the strongly emissive complex $\mathbf{DCa_2}$ (Fig. 5). The relatively weak fluorescence of complexes **DM** can be explained by the asymmetry of their electronic structure. It is known that the increase in the difference in the induction constants of 4,4′-substituents leads to the increase in the rate constant of photoinduced stilbene *trans–cis*-isomerization, which competes with radiative deactivation.[43]

Table 1 shows the values of equilibrium constants K_1, K_2 and K_S for the reactions with Ba^{2+} and Ca^{2+} ions, which are found by the nonlinear least squares method from spectrophotometric titration. The high values of stability constants are in good agreement with the previously found values for benzo-18-crown-6-ether derivatives.[44–46]

In spite of the difference between the diameter of the Ca^{2+} ion and the 18-membered macrocycle cavity size (the diameters of cations Ca^{2+}, Ba^{2+} and the 18-crown-6 macrocycle are equal to 1.98 Å, 2.68 Å and 2.6–3.2 Å, respectively), the binding constants of the Ca^{2+} ions with **D** and **DA** are not inferior to the binding constants of the Ba^{2+} ions (Table 1). Besides this, in both cases, the value of K_2 is less than that of K_1 due to electrostatic repulsion between the cations. The value of the stability constant of **DA** ($\log K_{DA} = 9.4 \pm 0.1$) is in good agreement with the values determined by other methods.[33,34]

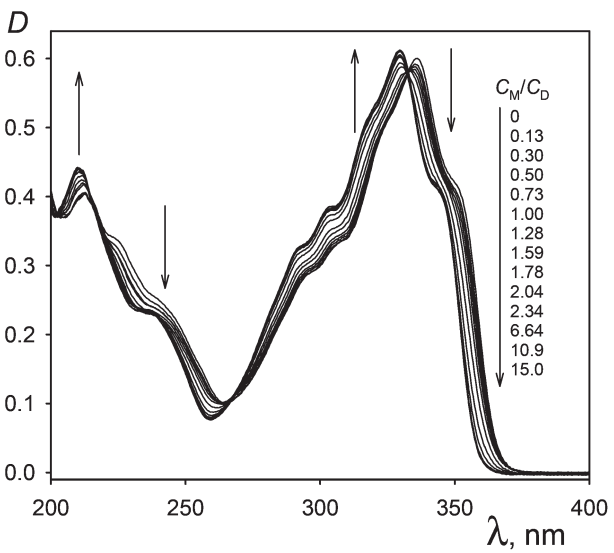

Fig. 4 The dependence of the absorption spectra of **D** ($C = 1.5 \times 10^{-5}$ M) in MeCN on the relative concentration of $Ba(ClO_4)_2$ (C_M/C_D varies from 0 to 15).

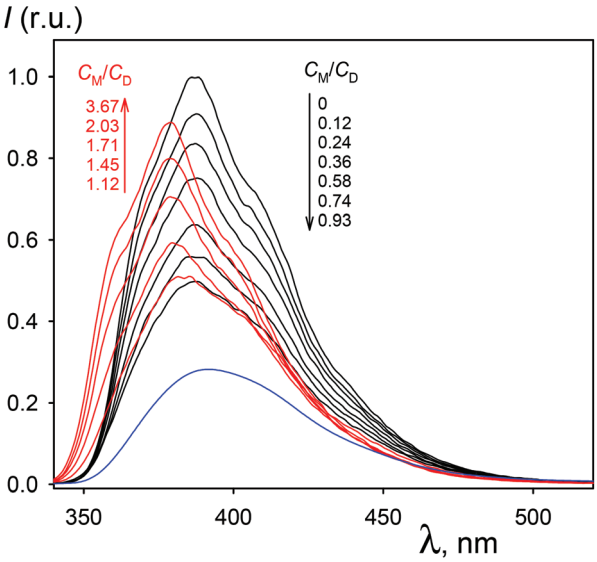

Fig. 5 Fluorescence spectra of **D** in MeCN ($C = 1.2 \times 10^{-5}$ M) with various relative concentrations of $Ca(ClO_4)_2$ (C_M/C_D varies from 0 to 3.7). The blue curve shows the calculated spectrum of the pure complex **DCa**.

Table 1 The values of equilibrium constants K_1, K_2 and K_S for the reactions with Ba^{2+} and Ca^{2+} ions in MeCN, and the calculated value K_{DA} obtained from eqn (3)

Ion	$\log K_1$, M^{-1}	$\log K_2$, M^{-1}	$\log K_S$, M^{-1}	$\log K_{DA}$, M^{-1}
Ba^{2+}	8.61	7.13	6.25	9.49
Ca^{2+}	8.52	7.08	6.33	9.27

Table 2 shows the spectral characteristics of **D**, **A**, **DA**, and of the complexes of **D** with Ba^{2+} and Ca^{2+} ions in MeCN. The complexation of **D** with Ba^{2+} and Ca^{2+} ions leads to a blue shift of the absorption maximum by 3–4 nm for **DM** and by 6 nm for $\mathbf{DM_2}$. In the latter case, the fluorescence spectrum maxima are also blue shifted by 7 nm. Contrary to this, the formation of complexes **DBa** and **DCa** leads to a red shift of the fluo-

Table 2 The values of absorption (λ_{abs}) and fluorescence (λ_{fl}) spectrum maxima, the molar extinction coefficient (ε) and the fluorescence quantum yield (φ) of **D**, **A**, **DA** and of the complexes of **D** with Ba^{2+} and Ca^{2+} ions in MeCN

	λ_{abs}, nm	ε, M^{-1} cm^{-1}	λ_{fl}, nm	φ
DA	533	340		<0.0001 (ref. 29)
	321	65 500		
D	336	37500 (ref. 29)	385	0.39
A	323	44 000	370	0.025
DBa	333	36 400	388	0.16
$\mathbf{DBa_2}$	330	38 100	378	0.34
DCa	332	36 600	388	0.15
$\mathbf{DCa_2}$	330	38 200	378	0.35

rescence spectrum maxima by 3 nm. This shift can point to the charge transfer in the excited states of **DM** due to their electronic asymmetry.

The issue of the stability of the complexes in organic solvent–water media is important for their practical applications. The decomposition of complexes **DA**, **DBa$_2$** and **DCa$_2$** in MeCN upon the addition of water was studied. Complexes **DBa$_2$** and **DCa$_2$** were obtained by adding a tenfold excess of barium and calcium perchlorates to the solution of **D**. The decomposition of the complexes in the presence of water can be described by using eqn (4)–(6),

$$M + nH_2O \overset{K_a}{\rightleftarrows} M{\cdot}nH_2O \quad (6)$$

where the stoichiometry of the aquacomplex is an optimizable parameter.

According to the spectrophotometric titration, optimal parameters are n = 2 and $\log K_a$ = 2.1 for complex **DBa$_2$** and n = 2 and $\log K_a$ = 2.6 for complex **DCa$_2$**. The half-decomposition of complex **DBa$_2$** at the first stage takes place when the water concentration is about 4 M (10%) and at the second stage when the water concentration is about 14 M (30%). The half-decomposition of complex **DCa$_2$** at the first stage takes place when the water concentration is about 2 M (5%) and at the second stage when the water concentration is about 10 M (20%).

When water is added to the solution of **DA** in MeCN, a gradual increase of an absorption band with the maximum at 324 nm and the shoulder at 336 nm is observed. This spectral form corresponds to an arithmetic sum of the free spectra of compounds **A** and **D**. The rank of the optical density matrix points to the presence of two absorbing components, which are **DA** and an equimolecular mixture of **D** and **A**. The decomposition of **DA** under the influence of water takes place according to eqn (7):

$$DA + nH_2O \overset{K_a}{\rightleftarrows} D + A{\cdot}nH_2O \quad (7)$$

The best description is achieved when n = 4 and $\log K_a$ = –7.1. The half-decomposition of **DA** takes place when the water concentration is about 3 M (7%).

Transient spectroscopy

In order to describe the evolution of transient spectra, the polyexponential model function (8) was used.

$$\Delta D(\lambda, t) = A_0(\lambda) + \sum_{i=1}^{n} A_i(\lambda) \exp\left(-\frac{t}{\tau_i}\right) \quad (8)$$

Here, $\Delta D(\lambda, t)$ is the differential optical density matrix, which depends on time t and wavelength λ; $A_0(\lambda)$ is the background vector, which does not depend on time, n is the number of exponents; $A_i(\lambda)$ is the vector of pre-exponential factors of the i-th exponent, which depends on wavelength; τ_i is the characteristic time of the i-th exponent. The characteristic times were found by the nonlinear least squares method, whereas the vectors of pre-exponential factors and the background vector were found by the linear least squares method.

Fig. 6 shows the dynamics of the transient spectra of **DA** ($C = 1 \times 10^{-4}$ M) after the pumping by using a 30 fs 330 nm laser pulse. The evolution of spectra is satisfactorily described by using eqn (8) for three exponents with characteristic times of 79 fs (**Ia**), 289 fs (**IIa**) and 397 fs (**IIIa**) (Fig. 7). The spectral contributions of each exponent are shown in the inset (Fig. 7). During the first 100 fs after the pumping, a rise of transient absorption (Fig. 6) takes place due to the component **Ia** with maxima of 425 nm and 535 nm by an absolute value (Fig. 7, inset). This process was referred to as the relaxation of the LE state. During the period between 100 fs and 400 fs, reshaping and a blue shift of spectra take place (Fig. 6, inset) due to the rising component **IIa** with a maximum of 492 nm.

This process was referred to as the conversion of the LE state into the CT state. Then, during the last 2 ps, a decay of transient absorption to the background level takes place due to the component **IIIa** with a maximum of 492 nm. This process was referred to as the conversion of the CT state into the ground state.

For the assignment of the vectors of pre-exponential factors, let us consider a series of transformations according to eqn (9).

$$LE_\nu \xrightarrow{k_0} LE \xrightarrow{k_1} CT \xrightarrow{k_2} GS \quad (9)$$

In eqn (9), k_0 is the monomolecular rate constant of the conversion of the initial LE$_\nu$ state into the relaxed LE state, k_1 is the monomolecular rate constant of the conversion of the relaxed LE state into the CT state, k_2 is the monomolecular rate constant of the conversion of the CT state into the ground state.

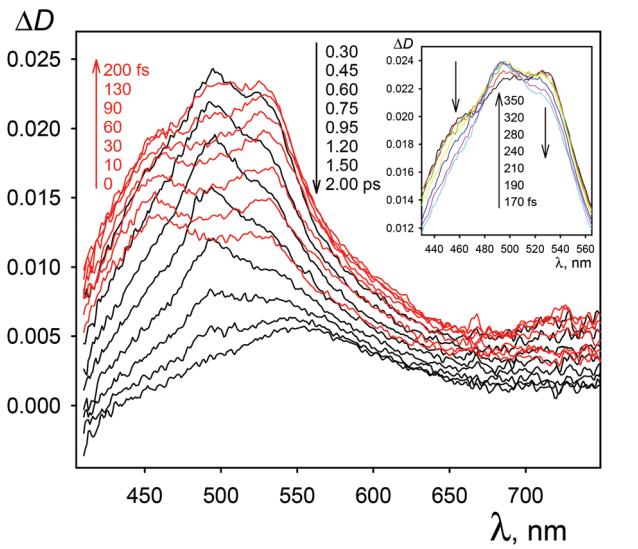

Fig. 6 The dynamics of the transient spectra of **DA**, which correspond to 10–200 fs delay times (red lines) and to 0.3–2.0 ps delay times (black lines), after the excitation by using a 30 fs 330 nm laser pulse. Inset: The reshaping of spectra during 170–350 fs delay times.

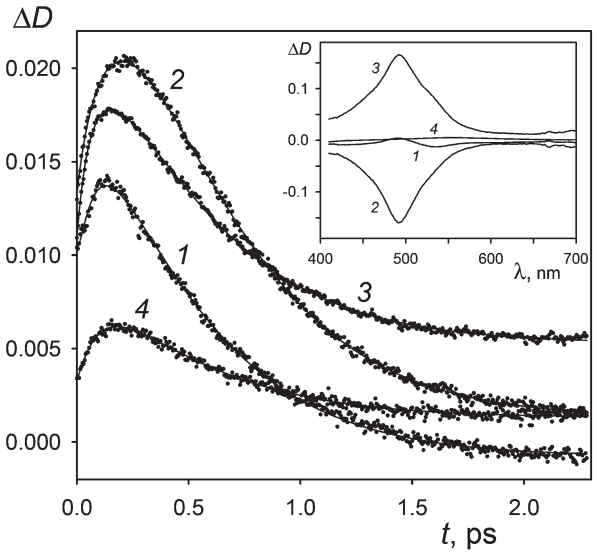

Fig. 7 The kinetics of the transient spectrum relaxation of **DA** after the excitation by using a 30 fs 330 nm laser pulse for several wavelengths: (1) 430 nm, (2) 470 nm, (3) 550 nm, and (4) 700 nm. The solid lines represent the data of three exponential models with characteristic times of 79 fs, 289 fs and 397 fs. Inset: The vectors of pre-exponential factors correspond to characteristic times: (1) 79 fs, (2) 289 fs, (3) 397 fs, and (4) background.

If the relaxation of the initial LE_ν state is taken as an instant process, the CT state will be the only intermediate product of transformations. Then, the dependence of the LE state concentration (C_{LE}) and of the CT state concentration (C_{CT}) on time t will be described by using eqn (10) and (11):

$$C_{LE} = C^0_{LE} e^{-k_1 t} \tag{10}$$

$$C_{CT} = \frac{k_1}{k_1 - k_2} C^0_{LE} (e^{-k_2 t} - e^{-k_1 t}) \tag{11}$$

Multiplying eqn (10) by ε_{LE}, and eqn (11) by ε_{CT}, and summing them, we can obtain eqn (12):

$$D = D_{LE} + D_{CT} = \left(\varepsilon_{LE} - \frac{k_1}{k_1 - k_2}\varepsilon_{CT}\right) C^0_{LE} e^{-k_1 t} + \\ + \frac{k_1}{k_1 - k_2}\varepsilon_{CT} C^0_{LE} e^{-k_2 t} \tag{12}$$

Here, D is the total optical density per length unity at a given wavelength, D_{LE} and D_{CT} are the optical densities of the LE and CT states, respectively, ε_{LE} and ε_{CT} are the molar extinction coefficients, C^0_{LE} is the initial concentration of the LE state. Taking into consideration the fact that $k_1 > k_2$, it follows from eqn (12) that the second vector of pre-exponential factors (Fig. 7, inset) is a linear combination of the inverted CT state absorption spectrum (about 80%) and of the LE state spectrum (about 20%). The characteristic time associated with the second vector corresponds to the process of conversion of the LE state into the CT state. In addition, it also follows from eqn (12) that the third vector (Fig. 7, inset) is a pure spectrum of the CT state. The characteristic time associated with the third vector corresponds to the process of deactivation of the CT state due to the back electron transfer. The first vector (Fig. 7, inset) corresponds to the fast process of accumulation of the relaxed LE state. This process was neglected while developing eqn (12).

Thus, the vectors of pre-exponential factors (Fig. 7, inset) have the following physical meaning. The first vector mainly corresponds to the inverted absorption spectrum of the LE state. The second vector mainly corresponds to the inverted absorption spectrum of the CT state. The third vector corresponds to the absorption spectrum of the CT state.

As is seen in Fig. 6, after the decay of absorption at 490 nm which takes place during the first 2 ps, the background signal retains at 555 nm. This background signal remains unchanged during the first tens of picoseconds. A similar background was also observed in ref. 29. Having a noticeable intensity as shown in Fig. 6, the background is rather weak as shown in Fig. 7 (inset). Based on the consideration of this background signal in a greater time period (500 ps), one can observe its slow decay (660 ps). In our opinion, this signal is not a photoproduct which could be formed as a result of fast photoprocesses. The position of the maximum and the large lifetime allow us to refer this background to small amounts of **D** as a result of the equilibrium dissociation of **DA**.

The kinetics of the LE_ν, LE and CT states according to eqn (9) is given in Fig. 8. The calculated absorption spectra of the pure LE and CT states (Fig. 8, inset) are similar to the first and third vectors of pre-exponential factors (Fig. 7, inset), respectively, as was expected.

In the picture, the shapes of the pre-exponential vectors correspond on the whole to the results of the previous work[29] for the analogue of **DA**, in which the bis(crown)stilbene molecule is separated from the molecule of a dipyridylethylene derivative by longer ammonioalkyl substituents, containing

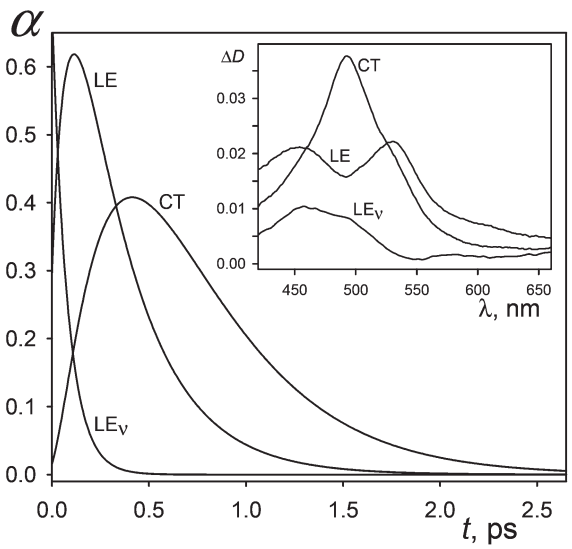

Fig. 8 The dependence of the molar fraction α of the LE_ν, LE and CT states on time t. The transient states are formed after the excitation of **DA** by using a 30 fs 330 nm laser pulse. Inset: The calculated spectra of the LE_ν, LE and CT states.

three methylene groups instead of two. The smaller value of the 79 fs fast rising exponent in comparison with the 150 fs exponent from the previous work[29] can be explained by the shorter duration of the exciting laser pulse. Similar values of the conversion time of the LE state into the CT state do not allow us to make a conclusion about the influence of the spatial structure of a donor–acceptor complex on these values. The time of back electron transfer (397 fs) is considerably less than the value (536 fs) obtained in the previous work.[29] This fact proves that the back electron transfer proceeds faster in a tighter complex. Since the ammonioethyl *N*-substituents in the acceptor molecule **A** are shorter as compared to ammoniopropyl substituents,[29] the distance between the two parallel planes of donor and acceptor molecules in complex **DA** is considerably less. This leads to a stronger overlap of their HOMO and LUMO molecular orbitals which is necessary for CTC formation. The tighter contact of donor and acceptor molecules results in a stronger upfield shift of acceptor proton signals in the ^{1}H-NMR spectra as well as in the bathochromic shift of the CT band in the optical spectra.[31]

In order to quantitatively take into account the effect of the spatial structure of **DA** on the electron transfer rate, we used the semiclassical single-mode nonadiabatic theory.[47] According to this theory, the rate of electron transfer in organic CTCs can be described as follows:

$$\frac{1}{\tau_{ET}} = H_{RP}^2\left(\frac{4\pi^3}{h^2\lambda_1 kT}\right)^{1/2}\sum_{n=0}^{\infty}\frac{S^n}{n!}\exp\left[-S-\frac{(\Delta G_0+\lambda_1+nh\nu_a)^2}{4\lambda_1 kT}\right],\quad S=\frac{\lambda_2}{h\nu_a} \tag{13}$$

Here, H_{RP} is the electronic coupling matrix element, ΔG_0 is the change in the Gibbs free energy, λ_1 is the reorganization energy associated with a solvent and low-frequency internal modes, λ_2 is the reorganization energy associated with the averaged frequency ν_a of high-frequency internal modes.

We used the following assumptions for comparing the experimental characteristic times of back electron transfer with the calculated values predicted from eqn (13). The estimation of the matrix element H_{PR} was performed by using the Hush formula:[48]

$$H_{RP} = \frac{0.0206}{r}\sqrt{\nu_{max}\Delta\nu_{1/2}\varepsilon_{max}} \tag{14}$$

Here, ν_{max}, $\Delta\nu_{1/2}$ and ε_{max} are the parameters of Gaussian, which approximates the CT band in the absorption spectrum of the complexes, r is the averaged distance between the donor and acceptor planes. The values of r were taken from the X-ray data.[34,49] It was found from the electrochemical data[27] that the value of ΔG_0 is a difference between the reduction potential of the acceptor (−0.43 eV) and the oxidation potential of the donor (1.24 eV), as components of a complex. As in ref. 29, the value of ν_a was equal to 1500 cm^{-1}. The internal temperature of the CT state was fixed at 300 *K*, assuming it to be close to room temperature.[29] The reorganization energy λ_2 was an optimizable parameter. The reorganization energy λ_1 was calculated from the complete reorganization energy λ_0 according to eqn (15):

$$\lambda_0 = \lambda_1 + \lambda_2 = \Delta G_0 + h\nu_{max} \tag{15}$$

Table 3 represents the values which were used for calculating the rates of back electron transfer according to eqn (13) for **DA** and its analogue with ammoniopropyl substituents.[29]

The tighter contact of the donor and the acceptor in **DA** as compared with that in its analogue leads to a 30% rise in the matrix element H_{RP} (Table 3). From this fact, one could expect an increase in the rate of electron transfer approximately by 1.6 times when passing from **DA** to its analogue. Besides this, in order to reconcile the experimental data with the values predicted from eqn (13), it is necessary to consider the reorganization energy λ_2 for **DA** (0.44 eV) about twice as big as that for its analogue (0.23 eV).

The spherical continual model[50] is often used to estimate the value of the solvent reorganization energy λ_1. According to this model,

$$\lambda_1 = \Delta q^2(d_D{}^{-1} + d_A{}^{-1} - r^{-1})(n^{-2} - \varepsilon^{-1}) \tag{16}$$

Here, Δq is the transferred charge value, d_D and d_A are the effective diameters of donor and acceptor molecules, respectively, r is the distance between them, n and ε are the refractive index and the dielectric permeability of the solvent, respectively. It is necessary to assume that d_D and d_A are equal to 5.9 Å and Δq is equal to 0.76 e for the agreement of eqn (16) with Table 3. Thus, the shortening of the ammonioalkyl substituent in **DA** as compared with the complex in ref. 29 leads to a decrease in the solvent reorganization energy λ_1.

The values obtained for the intramolecular reorganization energy λ_2 do not exceed the values obtained by resonance Raman spectroscopy for organic CTCs.[51,52] This fact indicates the applicability of the semiclassical single-mode nonadiabatic theory for describing photoelectron transfer in complex **DA**. The complex formation between bis(crown)stilbene and dipyridylethylene results in the suppression of vibration modes with frequencies less than 1634 cm^{-1} in Raman scattering

Table 3 Maximum position ν_{max}, bandwidth at half height $\Delta\nu_{1/2}$ and the intensity ε_{max} of the CT-band, distance between the donor and acceptor planes r, matrix element H_{RP}, change in the Gibbs free energy ΔG_0, low-frequency λ_1 and high-frequency λ_2 reorganization energies for **DA** and its analogue[29]

Bridge	ν_{max}, cm^{-1}	$\Delta\nu_{1/2}$, cm^{-1}	ε_{max}, M^{-1} cm^{-1}	r, Å	H_{RP}, eV	ΔG_0, eV	λ_1, eV	λ_2, eV
$(CH_2)_3$	19 700	4880	375	4.7	0.103	−1.67	0.54	0.23
$(CH_2)_2$	18 500	4880	331	3.4	0.130	−1.67	0.19	0.44

spectra of these compounds.[28,30] This indicates an increase in the rigidity of donor and acceptor moieties as a result of complex formation. It is known that the reorganization energy λ_2 is connected with the deformation of some chemical bonds.[53] The greater value of λ_2 for **DA** as compared with the complex in ref. 29 (Table 3) points to a bigger rigidity of **DA**.

Fig. 9 shows the dynamics of the transient spectra of **DA** ($C = 1 \times 10^{-2}$ M) after the pumping by using a 25 fs 580 nm laser pulse. The evolution of spectra is satisfactorily described by using eqn (8) for two exponents with characteristic times of 51 fs (**Ib**) and 417 fs (**IIb**) (Fig. 10). The spectral contributions of each exponent are shown in the inset (Fig. 10).

After the fast primary signal accumulation within the pulse duration (Fig. 9, inset), in the first 200 fs, reshaping and the shoulder decay at 470 nm (Fig. 9) take place due to the contribution of the component **Ib** with a maximum at 463 nm and a minimum at 492 nm. This process was referred to as the relaxation of the nonequilibrium CT state. Then, during the last 2 ps, a complete decay of the component **IIb** and the associated absorption band with a maximum at 492 nm is observed. This process was referred to as the conversion of the CT state into the ground state.

The CT state lifetimes obtained under 330 nm and 580 nm excitation are in good agreement with one another. The first vector of pre-exponential factors (Fig. 10, inset) corresponds to the superposition of the absorption spectra of nonequilibrated and relaxed CT states. The second vector is a pure absorption spectrum of the relaxed CT state.

Scheme 1 summarizes the processes which take place upon the excitation of **DA** at the main absorption band and at the CT band.

We also studied the dynamics of singlet excited states of bis(crown)stilbene **D** and its complexes **DBa** and $\mathbf{DBa_2}$ in MeCN.

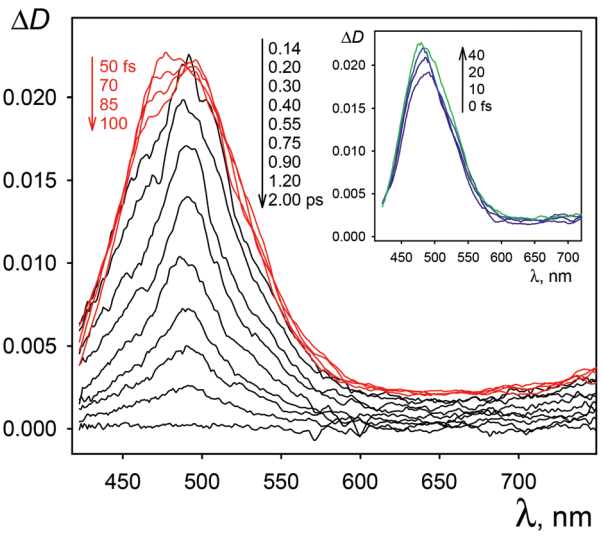

Fig. 9 The dynamics of the transient spectra of **DA**, which correspond to 50–100 fs delay times (red lines) and to 0.14–2.0 ps delay times (black lines), after the excitation by using a 25 fs 580 nm laser pulse. Inset: The dynamics of the spectra, which correspond to 0–40 fs delay times.

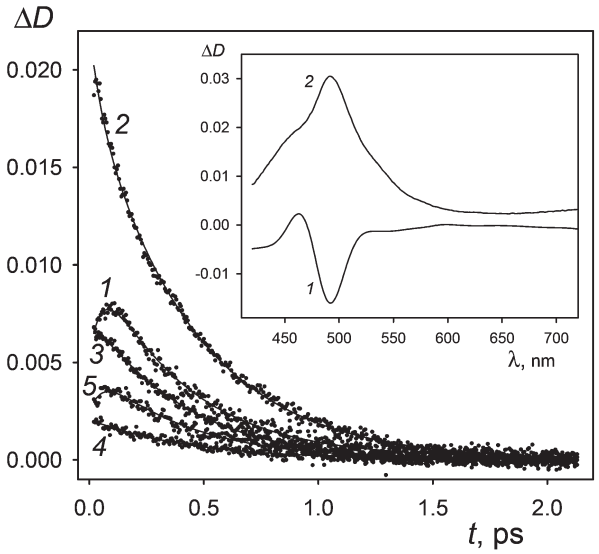

Fig. 10 The kinetics of the transient spectrum relaxation of **DA** after the excitation by using a 25 fs 580 nm laser pulse for several wavelengths: (1) 430 nm, (2) 460 nm, (3) 550 nm, (4) 640 nm, and (5) 780 nm. The solid lines represent the data of two exponential models with characteristic times of 51 fs and 417 fs. Inset: The vectors of pre-exponential factors correspond to characteristic times: (1) 51 fs and (2) 417 fs.

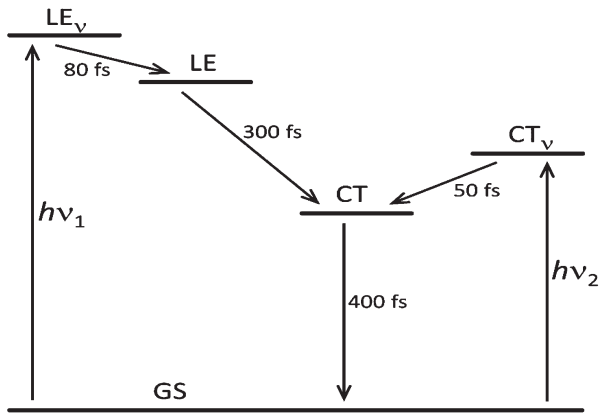

Scheme 1 Processes upon the excitation of **DA** at the main absorption band ($h\nu_1$) and at the CT band ($h\nu_2$).

The solutions of **DBa** and $\mathbf{DBa_2}$ were prepared by adding barium perchlorate to the solution of **D** ($C = 5 \times 10^{-4}$ M) in an equimolar amount and fivefold excess, respectively. The equilibrium content of complex **DBa** was about 60%, whereas the content of complex $\mathbf{DBa_2}$ was almost 100%. In all the three cases, the dynamics of transient spectra is described in a similar way. During the first 500 fs, a rise in the absorption intensity takes place. After that, the shapes and the positions of the spectra do not change with time and the maxima of transient spectra retain their positions at 558 nm, 562 nm and 569 nm for the solutions of **D**, **DBa** and $\mathbf{DBa_2}$, respectively. The intensity of spectra slowly decays according to the monoexponential law with characteristic times of 640 ps, 470 ps and

597 ps, respectively. The data obtained indicate that the lifetime of the excited molecule of **D** decreases upon binding with one cation due to the asymmetry of the electronic structure of the resulting complex.

Conclusion

Thermodynamic and kinetic properties of the charge transfer complex **DA** between (*E*)-bis(18-crown-6)stilbene and 4,4′-(*E*)-ethene-1,2-diylbis[1-(2-ammonioethyl)pyridinium]tetraperchlorate were studied in ground and excited electron states by means of steady-state absorption and fluorescence spectroscopy, as well as femtosecond transient absorption spectroscopy.

The characteristic time of back electron transfer in the CT state of **DA** was determined by femtosecond transient absorption spectroscopy upon excitation at the 330 nm or 580 nm band is the same, and is equal to 410 ± 20 fs. This value is smaller than that was found previously for analogous CTCs but with longer ammonioalkyl substituents (540 ± 30 fs).[29] This result can be explained by using the tighter spatial structure of **DA** as compared with the analogous complex,[29] which leads to a stronger electronic coupling between the donor and the acceptor within a complex.

Complex **DA** does not fluoresce due to fast subpicosecond photoinduced reactions of direct and back electron transfer. The direct electron transfer leads to the conversion of the locally excited electron state into the charge transfer (CT) state. The back electron transfer leads to the deactivation of the CT state to the ground state.

Upon the interaction of **DA** with alkaline-earth metal cations a "switch-on" of **DA** fluorescence takes place due to the substitution of the acceptor molecule by two metal cations and the suppression of electron transfer processes. In this case the disappearance of the charge transfer absorption band is also observed. Complex **DA** can therefore be considered as a promising supramolecular optical sensor for the determination of metal cations.

Conflicts of interest

There are no conflicts to declare.

Acknowledgements

This work was supported by the Russian Science Foundation (in respect of organic synthesis, project no. 14-13-00076) and by the Russian Foundation for Basic Research (project no. 17-03-00595).

References

1 S. Fery-Forgues and F. Al-Ali, Bis(azacrown ether) and bis(benzocrown ether) dyes: butterflies, tweezers and rods in cation binding, *J. Photochem. Photobiol., C*, 2004, **5**, 139–153.
2 M. Nakamura, H. Yokono, K. Tomita, M. Ouchi, M. Miki and R. Dohno, Substitution effect, absorption, and fluorescence behaviors of 11,12-benzo-1,7,10,13-tetraoxa-4-azacyclopentadec-11-ene (benzoaza-15-crown-5) derivatives upon cation complexation in solvent extraction, *J. Org. Chem.*, 2002, **67**, 3533–3536.
3 J. S. Bradshaw, R. M. Izatt and Zh. Yan, Bis- and oligo (benzocrown ether)s, *Chem. Rev.*, 1994, **94**, 939–991.
4 K. Kikukawa, G.-X. He, A. Abe, T. Goto, R. Arata, T. Ikeda, F. Wada and T. Matsuda, New applications of crown ethers. Part 6. Structural effects of bis(benzocrownether)s and substituted benzocrown ethers on solvent extraction and complexation of alkali-metal cations, *J. Chem. Soc., Perkin Trans. 2*, 1987, 135–141.
5 S. Shinkai, K. Shigematsu, Yu. Kusano and O. Manabe, Photoresponsive crown ethers. Part 3. Photocontrol of ion extraction and ion transport by several photofunctional bis (crown ethers), *J. Chem. Soc., Perkin Trans. 1*, 1981, 3279–3283.
6 S. Shinkai, K. Shigematsu, M. Sato and O. Manabe, Photoresponsive crown ethers. Part 6. Ion transport mediated by photoinduced cis-trans interconversion of azobis(benzocrown ethers), *J. Chem. Soc., Perkin Trans. 1*, 1982, 2735–2739.
7 S. Shinkai, T. Ogawa, Yu. Kusano, O. Manabe, K. Kikukawa, T. Goto and Ts. Matsuda, Photoresponsive crown ethers. 4. Influence of alkali metal cations on photoisomerization and thermal isomerization of azobis(benzocrown ether)s, *J. Am. Chem. Soc.*, 1982, **104**, 1960–1967.
8 A. Kumano, O. Niwa, T. Kajiyama, M. Takayanagi, K. Kano and S. Shinkai, Photoinduced ion permiation through ternary composite membrane composed of polymer/liquid crystal/azobenzene-bridged crown ether, *Chem. Lett.*, 1983, 1327–1330.
9 M. Takeshita and M. Irie, Photoresponsive tweezers for alkali metal ions. Photochromic diarylethenes having two crown ether moieties, *J. Org. Chem.*, 1998, **63**, 6643–6649.
10 S. H. Kawai, Photochromic bis(monoaza-crown ether)s. Alkali-metal cation complexing properties of novel diarylethenes, *Tetrahedron Lett.*, 1998, **39**, 4445–4448.
11 K. Kimura, R. Mizutani, M. Yokoyama, R. Arakawa and Y. Sakurai, Metal-ion complexation and photochromizm of triphenylmethane dye derivatives incorporating monoaza-15-crown-5 moieties, *J. Am. Chem. Soc.*, 2000, **122**, 5448–5454.
12 K. Kimura, G. Yokota, M. Yokoyama and R. M. Uda, Cation complexation and photochromism of copolymers carrying pendant crowned malachite green moiety, *Macromol.*, 2001, **34**, 2262–2268.
13 E. N. Ushakov, S. P. Gromov, A. I. Vedernikov, E. V. Malysheva, A. A. Botsmanova, M. V. Alfimov, B. Eliasson, U. G. Edlund, J. K. Whitesell and M. A. Fox, Self-organization of highly stable electron donor-acceptor complexes via host-guest Interactions, *J. Phys. Chem. A*, 2002, **106**, 2020–2023.

14 A. P. Hansson, P.-O. Norrby and K. Wärnmark, A bis(crown-ether) analogue of Tröger's base: Recognition of achiral and chiral primary bisammonium salts, *Tetrahedron Lett.*, 1998, **39**, 4565–4568.
15 E. V. Lukovskaya, A. A. Kosmacheva, O. A. Fedorova, A. A. Bobyleva, A. V. Dolganov, N. E. Shepel', Yu. V. Fedorov, V. V. Novikov and A. V. Anisimov, Synthesis of chromophoric crown-containing styryl derivative of terthiophene and Its complexation with octane-1,8-diaminium diperchlorate, *Russ. J. Org. Chem.*, 2014, **50**, 552–558.
16 S. P. Gromov, A. I. Vedernikov, N. A. Lobova, L. G. Kuz'mina, S. S. Basok, Yu. A. Strelenko, M. V. Alfimov and J. A. K. Howard, Controlled self-assembly of bis(crown) stilbenes into unusual bis-sandwich complexes: structure and stereoselective [2 + 2] photocycloaddition, *New J. Chem.*, 2011, **35**, 724–737.
17 S. P. Gromov, A. I. Vedernikov, L. G. Kuz'mina, N. A. Lobova, S. S. Basok, Yu. A. Strelenko and M. V. Alfimov, Stereoselective [2 + 2] photocycloaddition in bispseudosandwich complexes of bis(18-crown-6) stilbene with alkanediammonium ions, *Russ. Chem. Bull.*, 2009, **58**, 108–114.
18 P. L. Anelli, N. Spencer and J. F. Stoddart, Diazadibenzo-30-crown-10 derivatives as receptors for diquat, *Tetrahedron Lett.*, 1988, **29**, 1569–1572.
19 T. Nabeshima and D. Nishida, Control of binding affinity to paraquat by novel macrocyclic systems responding to redox reactions, *Tetrahedron Lett.*, 2002, **43**, 5719–5722.
20 F. Huang, L. N. Zakharov, A. L. Rheingold, M. Ashraf-Khorassani and H. W. Gibson, Synthesis of a symmetric cylindrical bis(crown ether) host and its complexation with paraquat, *J. Org. Chem.*, 2005, **70**, 809–813.
21 F. Huang, P. Gantzel, D. S. Nagvekar, A. L. Rheingold and H. W. Gibson, Taco grande: a dumbbell bis(crown ether)/paraquat [3](taco complex), *Tetrahedron Lett.*, 2006, **47**, 7841–7844.
22 M. Zhang, K. Zhu and F. Huang, Improved complexation of paraquat derivatives by the formation of crown ether-based cryptands, *Chem. Commun.*, 2010, **46**, 8131–8141.
23 R. S. Forgan, Ch. Wang, D. C. Friedman, J. M. Spruell, Ch. L. Stern, A. A. Sarjeant, D. Cao and J. F. Stoddart, Donor–acceptor ring-in-ring complexes, *Chem. – Eur. J.*, 2012, **18**, 202–212.
24 T. Kuwabara, M. Sugiyama, K. Takeuchi and H. Sakane, Catenane and inclusion complex as photochromic compounds involving viologen units, *J. Photochem. Photobiol., A*, 2013, **269**, 59–64.
25 H. W. Gibson, Ya Xi Shen, M. C. Bheda and C. Gong, Polymeric molecular shuttles: Polypseudorotaxanes & polyrotaxanes based on viologen (paraquat) urethane backbones & bis(p-phenylene)-34-crown-10, *Polymer*, 2014, **55**, 3202–3211.
26 S. P. Gromov, E. N. Ushakov, A. I. Vedernikov, N. A. Lobova, M. V. Alfimov, Yu. A. Strelenko, J. K. Whitesell and M. A. Fox, A novel optical sensor for metal ions based on ground-state intermolecular charge-transfer complexation, *Org. Lett.*, 1999, **1**, 1697–1699.
27 K. P. Butin, A. A. Moiseeva, S. P. Gromov, A. I. Vedernikov, A. A. Botsmanova, E. N. Ushakov and M. V. Alfimov, Prospects of electroanalytical investigations of supramolecular complexes of a bis-crown stilbene with viologen-like compounds bearing two ammonioalkyl groups, *J. Electroanal. Chem.*, 2003, **547**, 93–102.
28 I. S. Alaverdian, A. V. Feofanov, S. P. Gromov, A. I. Vedernikov, N. A. Lobova and M. V. Alfimov, Structure of charge-transfer complexes formed by biscrown stilbene and dipyridylethylene derivatives as probed by surface-enhanced Raman scattering spectroscopy, *J. Phys. Chem. A*, 2003, **107**, 9542–9546.
29 E. N. Ushakov, V. A. Nadtochenko, S. P. Gromov, A. I. Vedernikov, N. A. Lobova, M. V. Alfimov, F. E. Gostev, A. N. Petrukhin and O. M. Sarkisov, Ultrafast excited state dynamics of the bi- and termolecular stilbene-viologen charge-transfer complexes assembled via host–guest interactions, *Chem. Phys.*, 2004, **298**, 251–261.
30 Yu. S. Alaverdyan, A. V. Feofanov, S. P. Gromov, A. I. Vedernikov, N. A. Lobova and M. V. Alfimov, Spectroscopy of surface-enhanced Raman scattering of a complex with charge transfer between a bis-crown-containing stilbene and a bis-ammonium-alkyl derivative of dipyridylethylene, *Opt. Spectrosc.*, 2004, **97**, 560–566.
31 S. P. Gromov, A. I. Vedernikov, E. N. Ushakov, N. A. Lobova, A. A. Botsmanova, L. G. Kuz'mina, A. V. Churakov, Yu. A. Strelenko, M. V. Alfimov, J. A. K. Howard, D. Johnels and U. G. Edlund, Novel supramolecular charge-transfer systems based on bis(18-crown-6)stilbene and viologen analogues bearing two ammonioalkyl groups, *New J. Chem.*, 2005, **29**, 881–894.
32 A. I. Vedernikov, L. G. Kuz'mina, N. A. Lobova, E. N. Ushakov, J. A. K. Howard, M. V. Alfimov and S. P. Gromov, Unusual three-decker structure of a D–A–D complex between bis(crown)stilbene and a di(quinolyl) ethylene derivative, *Mendeleev Commun.*, 2007, **17**, 151–153.
33 S. P. Gromov, A. I. Vedernikov, E. N. Ushakov and M. V. Alfimov, Unusual supramolecular donor-acceptor complexes of bis(crown)stilbenes and bis(crown)azobenzene with viologen analogs, *Russ. Chem. Bull.*, 2008, **57**, 793–801.
34 A. I. Vedernikov, E. N. Ushakov, A. A. Efremova, L. G. Kuz'mina, A. A. Moiseeva, N. A. Lobova, A. V. Churakov, Yu. A. Strelenko, M. V. Alfimov, J. A. K. Howard and S. P. Gromov, Synthesis, structure, and properties of supramolecular charge-transfer complexes between bis(18-crown-6)stilbene and ammonioalkyl derivatives of 4,4′-bipyridine and 2,7-diazapyrene, *J. Org. Chem.*, 2011, **76**, 6768–6779.
35 A. I. Vedernikov, S. S. Basok, S. P. Gromov, L. G. Kuz'mina, V. G. Avakyan, N. A. Lobova, E. Yu. Kulygina, T. V. Titkov, Yu. A. Strelenko, E. I. Ivanov, J. A. K. Howard and M. V. Alfimov, Synthesis and structure of bis-crown-containing stilbenes, *Russ. J. Org. Chem.*, 2005, **41**, 843–854.
36 W. H. Melhuish, Quantum efficiencies of fluorescence of organic substances – effect of solvent and concentration of fluorescence solute, *J. Phys. Chem.*, 1961, **65**, 229–235.

37 V. V. Volchkov, F. E. Gostev, I. V. Shelaev, V. A. Nadtochenko, S. N. Dmitrieva, S. P. Gromov, M. V. Alfimov and M. Ya. Melnikov, Complexation of donor-acceptor substituted aza-crowns with alkali and alkaline earth metal cations. Charge transfer and recoordination in excited state, *J. Fluoresc.*, 2016, **26**, 585–592.

38 M. V. Rusalov, Numerical simulation of chemical equilibria and photostationary states using spectrophotometric and spectrofluorometric data, *Russ. J. Gen. Chem.*, 2005, **75**, 351–358.

39 T. Kuwabara, H. Guo and H. Orii, Guest-responsive intramolecular charge transfer of viologen-crown ether conjugate, *Tetrahedron Lett.*, 2012, **53**, 5099–5101.

40 G. Lindsten, O. Wannerstörm and B. Thuin, Stilbene biscrown ether: synthesis, complexation and photoisomerization, *Acta Chem. Scand., Ser. B*, 1986, **40**, 545–553.

41 E. N. Ushakov, T. P. Martyanov, A. I. Vedernikov, O. V. Pikalov, A. A. Efremova, L. G. Kuz'mina, J. A. K. Howard, M. V. Alfimov and S. P. Gromov, Self-assembly through hydrogen bonding and photochemical properties of supramolecular complexes of bis(18-crown-6) stilbene with alkanediammonium ions, *J. Photochem. Photobiol., A*, 2017, **340**, 80–87.

42 R. M. Wallace and S. M. Katz, A method for the determination of rank in the analysis of absorption spectra of multicomponent systems, *J. Phys. Chem.*, 1964, **68**, 3890–3892.

43 V. Papper, D. Pines, D. G. Likhtenshtein and E. Pines, Photophysical characterization of trans-4,4′-disubstituted stilbenes, *J. Photochem. Photobiol., A*, 1997, **111**, 87–96.

44 I. Leray, J.-L. Habib-Jiwan, C. Branger, J.-Ph. Soumillion and B. Valeur, Ion-responsive fluorescent compounds VI. Coumarin 153 linked to rigid crowns for improvement of selectivity, *J. Photochem. Photobiol., A*, 2000, **135**, 163–169.

45 T. P. Martyanov, E. N. Ushakov, V. A. Savelyev and L. S. Klimenko, Crown-containing naphtho- and anthraquinones: synthesis and complexation with alkali and alkaline-earth metal cations, *Russ. Chem. Bull.*, 2012, **61**, 2282–2294.

46 J. Massaux, G. Roland and J. F. Desreux, On the complexation of alkaline earth metal cations in propylene carbonate by macrocyclic crown ethers featuring from four to ten coordinating sites, *Inorg. Chim. Acta*, 1982, **60**, 129–133.

47 B. S. Brunschwig and N. Sutin, Rate-constant expressions for nonadiabatic electron-transfer reactions, *Comments lnorg. Chem.*, 1987, **6**, 209–235.

48 P. F. Barbara, Th. J. Meyer and M. A. Ratner, Contemporary issues in electron transfer research, *J. Phys. Chem.*, 1996, **100**, 13148–13168.

49 A. I. Vedernikov, L. G. Kuz'mina, A. A. Botsmanova, Yu. A. Strelenko, J. A. K. Howard, M. V. Alfimov and S. P. Gromov, Stacking structures of complexes between bis(crown)azobenzene and a dipyridylethylene derivative in a crystal and in solution, *Mendeleev Commun.*, 2007, **17**, 148–150.

50 C. Prayer, T.-H. Tran-Thi, S. Pommeret, P. d'Oliveira and P. Meynadier, Light- and pH-driven electron transfer in the pyranine–methylviologen system, *Chem. Phys. Lett.*, 2000, **323**, 467–473.

51 D. L. Phillips, I. R. Gould, J. W. Verhoeven, D. Tittelbach-Helmrich and A. B. Myers, Resonance Raman analysis of charge-transfer reorganization energies in a covalent dicyanoethylene-aza-adamantane, *Chem. Phys. Lett.*, 1996, **258**, 87–93.

52 F. Markel, N. S. Ferris, I. R. Gould and A. B. Myers, Mode-Specific Vibrational Reorganization Energies Accompanying Photoinduced Electron Transfer in the Hexamethylbenzene/Tetracyanoethylene Charge-Transfer Complex, *J. Am. Chem. Soc.*, 1992, **114**, 6208–6219.

53 R. G. Hadt, X. Xie, S. R. Pauleta, I. Moura and E. I. Solomon, Analysis of resonance Raman data on the blue copper site in pseudoazurin: Excited state π and σ charge transfer distortions and their relation to ground state reorganization energy, *J. Inorg. Biochem.*, 2012, **115**, 155–162.